

Saad T. Hamidi

Electromechanical
Engineering Department,
University of Technology,
Baghdad, Iraq.
11007@uotechnology.edu.iq

Received on: 29/06/2019
Accepted on: 21/08/2019
Published online: 25/11/2019

An Experimental Investigation on Thermal Efficiency of Flat Plate Tube Solar Collector using Nanofluid with Solar Tracking Mechanism

Abstract- In the present work, flat-plate solar collector (FPSC) in terms of various parameters as well as in respect of lower (Area of FPSC, volume fraction concentration of nanofluids, and mass flow rate) has been studied in this work. The FPSC has been fabricated with 0.192 m^2 , Dioxide silicon SiO_2 (40nm) with the volume fraction of SiO_2 +Distilled water (0.05, 0.075, and 0.1%) and varying of flow rate (10, 15, 20L/h). These technological devices operate under forced circulation mode of fluid under varying climate conditions. The tracking mechanism has been used in the experiment of FPSC for tracking the sun position during the daytime. As per the ASHRAE standard. The results showed that at volume fraction 0.10 % and flow rate of 20 L/h, the highest increase in the absorbed energy parameter $F_R(\tau\alpha)$ was 7.3 %, and the removed energy parameter $F_R U_L$ was 11.9 % compared with distilled water. The changes in absorbed energy parameter $F_R(\tau\alpha)$ they vary from 4.4% to 7.3% while in removed energy parameter $F_R U_L$, the vary from 1.3% to 11.9% as compared with the distilled water case. The maximum efficiency was about 70 % as the decreased temperature parameter $[(T_i - T_a)/G_T]$ is equal to zero at a volume fraction of 0.10 % and flow rate of 20 L/h.

Keywords- Flat plate solar collector; thermal efficiency; SiO_2 /water Nanofluids

How to cite this article: S.T. Hamidi, "An Experimental Investigation on Thermal Efficiency of Flat Plate Tube Solar Collector using Nanofluid with Solar Tracking Mechanism," *Engineering and Technology Journal*, Vol. 37, No. 11, pp. 475-487, 2019.

1. Introduction

One of the cleanest forms of renewable energy sources is solar energy. The most common method to employ solar energy is to utilize a solar energy collector. Flat-plate collectors FPSCs are the most commonly utilized type of solar collector as to the heater, the water, or air. Those collectors have distinguished by low outlet temperature and efficiency [1-8]. Lately, many researchers tried enhancing the performance and efficiency of the FPSC by using several techniques. One of these techniques is to use nanofluids in solar collectors instead of commonly used liquids [9–13]. The researchers [14,15] studied the effects of environmental, thermal, and economical use of nanofluids for improving solar collector efficiency. Youssef et al. [16] who had been tested a coolant of $\text{Al}_2\text{O}_3/\text{H}_2\text{O}$ as a coolant in a FPSC. They have proven that the nanofluids have raised the temperature outlet and collector efficiency.

The performance of a mini-channel solar energy collector had been evaluated with four different nanofluids by Mahian et al. [17]. The nanofluids were $\text{Al}_2\text{O}_3/\text{H}_2\text{O}$, $\text{TiO}_2/\text{H}_2\text{O}$, $\text{SiO}_2/\text{H}_2\text{O}$, and $\text{Cu}/\text{H}_2\text{O}$. They concluded that coolant $\text{Cu}/\text{H}_2\text{O}$ is

the best nanofluid, which provides the highest outlet-temperature and lowest entropy. Verma et al. [18] carried out an experimental investigation on a FPSC with variety of nanofluids with regarding various parameters concerning energy and energy efficiency. Experimental test results deduced that volumetric concentration about 0.75% at a rated flow of 0.025 kg/sec might cause optimal energy efficiency. Faizal et al. [19] conducted studies to save the necessary material for manufacturing solar collectors, in addition to reduce energy consumption for every collector fabrication. This study showed that it is possible to reduce the solar collector area by 21.6%, 25.6%, 21.5% & 22.1% with SiO_2 , CuO , Al_2O_3 , and TiO_2 , respectively. Alim et al. [20] carried out a theoretical study for analyzing the consequences on entropy generation, the ability to enhance heat transfer in addition to pressure drop with various types of nanofluids like CuO , TiO_2 , Al_2O_3 and SiO_2 with water as fluid at different values of rates the flow in a FPSC. The remarkable drawn results of the investigation showed that the enhanced heat transfer was 22.15% with low heat generation 4.34% comparing with pure water as working fluid.

Arıkan et al. [21] have studied the influence of ZnO-H₂O, Al₂O₃-H₂O nanofluids, with/without ethylene glycol (EG), on the FPSC efficiency. They build two systems and at the same time, examined the nanofluids with /without EG on the PSC efficiency. The volume fraction of EG and nanoparticles were 0.25% and 25%, respectively. Three mass flow rates were used in this study: 0.05 kg/s, 0.07 kg/s & 0.09 kg/s. ASHRAE Standard 93-2010 had been utilized to determine system efficiency. The efficiency of the collector was compared with the base fluid (distilled water). The experimental results also showed that increasing the mass flow rate and use EG led to increasing the system efficiency. Moreover, there was a great increase in efficiency by (15.13%) at 0.09 kg/s when utilizing nanofluid Al₂O₃-H₂O/EG as compared with the base liquid. Tiwari et al. [22] theoretically investigated the influence of utilizing Al₂O₃ nanofluid as the medium of absorption on the performance of a FPSC. The study also addressed the impact of particle size fraction and mass flow rate on collector efficiency. The results proved that employing the optimum particle size fraction of 1.5% for Al₂O₃ nanofluid will increase the solar collector thermal efficiency by 31.64% as compared with distilled water as the working fluid. Golden et al. [23] provided empirical results on solar collectors based on nanofluid, which includes a variety of nanoparticles (carbon nanotubes and graphite, silver). Efficiency enhancements in thermal solar collectors using nanofluids as a mechanism to absorb have reached 5%. Experimental and numerical findings showed a quick initial raise in the efficiency with volume fraction, followed when by a decline in efficiency as volume fraction continues increasing.

Many scientists have employed the solar tracking system to improve the solar collector system performance further. Rhushi et al. [24] presented an experimental analysis of a FPSC and introduced a comparison of performance with or without using a tracking system. The commercial 100 liter/day flat plate water heater has been built and developed into a testing-rig to carry out the experimental setup.

Experimental tests were carried out on the FPSC in almost identical weather conditions for a week, and data were collected from both cases, the use

of the tracking system or without. The results showed a 40°C average increase in the outlet temperature. It has been calculated the efficiency of two conditions, and the comparison proved that there is a rise of 21 % in the efficiency. Drago [25] had compared the energy gain of four flat-panel collectors. Two collectors were mounted: one has a single cover, and the other has double covers while the other two solar collectors have combined with full tracking system. The experimental results demonstrated that the efficiencies for the single cover with and without using tracking were 5.7 % and 10.1 %, respectively, while in double cover were 17.4 % and 21.8 %, respectively. Pavelet et al. [26] analyzed theoretically and experimentally the collected energy with and without using a tracking mechanism with bifacial and non-bifacial photovoltaic PV solar systems. The calculated and measured tracking influence proved that there was an increase in collected energy by 30 – 40 % using bifacial panels without tracking action, and projecting reflector collecting solar radiation on the back had given rise in the collected solar energy around 50 – 60 % with the same panel. It noted in this day that the use of nanofluid technology rather than traditional liquids is a potential area where the performance of the solar energy collectors might be enhanced. The nanofluid selection process is a very significant factor in the solar collector. The nanofluids have some limitation i.e., erosion and corrosion of components, pressure drop, high cost, pumping power problem, conventional heat transfer fluids.

2. Experimental Methodology

1. Main Components

Figure 1 detailed photograph showing the various components involved in the experimental work. Construction of the FPSC is modified [27] to application in this experimental work. Figure 1 with specifications listed in Table 1. Dioxide silicon SiO₂ (40nm) + Distilled water (DW), based nanofluid of volume fraction concentration of 0.05% , 0.075%, and 0.10%, as working fluid is fabricated to flow through the collector at different values of flow rates of 10L/h, 15L/h and 20L/h.



Figure 1: Schematic of flat-plate solar collector

Table 1: Specification of flat-plate solar collector

Parameter	Parameter	Parameter	Parameter
Number of pipes	4	Thickness of absorber plate	0.015 m
Length of copper pipe	0.64 m	Number of glass cover	1
Outer diameter of cooper pipe	0.018 m	Thickness of glass cover	0.004 m
Thickness of copper pipe	0.002 m	Thickness of insulation	0.05 m
Outer diameter of header	0.03 m	Length of frame	0.78 m
Distance between pipes	0.08	Width of frame	0.39
Length of absorber plate	0.60 m	Thickness of frame	0.002 m
Width of absorber plate	0.320 m	Tracking mechanism	One-axis

II. Tracking mechanism

In general, solar tracking could be represented by two modes: one-axis tracking and two-axis tracking. The one-axis tracking of the FPSC system could be orientated in the north-south direction to track the sun from the east to west [27], while in the two-axis tracking system, the collector follows both of the sun's changing altitude and azimuth. The mechanical system includes the main structure that supports the solar collector, providing one degree of freedom (the movement in one direction). A lightweight

steel structure was built to provide a reliable mechanical support against high wind speed and harsh environmental conditions. The mechanical system consists of a fixed part and a moving part. The fixed part is very important to fix the FPSC system, called the base. The moving part of moving the FPSC from east to west to track the sunrays, this movement can be directed by using a manual tracking mechanism used for this experiment to track the sun position during the day is shown in Figure 2.



Figure 2: Schematic of Mechanism of tracking of the FPSC

III Nanofluid

a. Nanofluid Preparation

Before preparing the Nanofluids, it is very necessary to measure the weight of SiO_2 nanoparticles required in water for varying

concentrations, byemploying the typical expression [28].

$$\varphi \% = \frac{\frac{W_{np}}{\rho_{np}}}{\frac{W_{np}}{\rho_{np}} + \frac{W_{bf}}{\rho_{bf}}} \times 100$$

(1)

Where:

φ – the volume fraction concentration, W_{np} – weight of nanoparticles (kg)

ρ_{np} – the density of nanoparticles (kg/m³), W_{bf} – weight base fluid (ml)

ρ_{bf} - the density of the base fluid (kg/m³)

The weight of nanoparticles is measured in grams by using a digital weighing machine shown in Figure 3a, through mixing nanoparticles of SiO₂ in 1000 ml of distilled water to make the volume

concentration (φ) of 0.05%, 0.075%, and 0.10%, respectively. Now, stirring is done by putting a small amount of SiO₂ nanoparticles in 1000 ml of distilled water to make the volumetric concentration, continuously for about 30 minutes on the magnetic stirrer with hot plate system, figure 3b. In order to get more stable and more widespread nanoparticles in the water, and ultra sonicator could be used. The solution then put on the sonicator figure 3c and sonication is done for three hours, to be the nanofluid ready the applied and figure 4, show the prepared sample of 0.05%, 0.075%, and 0.10% By vol.conc.SiO₂+H₂O, respectively.



Figure 3a: Digital weigh Figure 3b: Magnetic stirrer Figure 3c: Sonicator

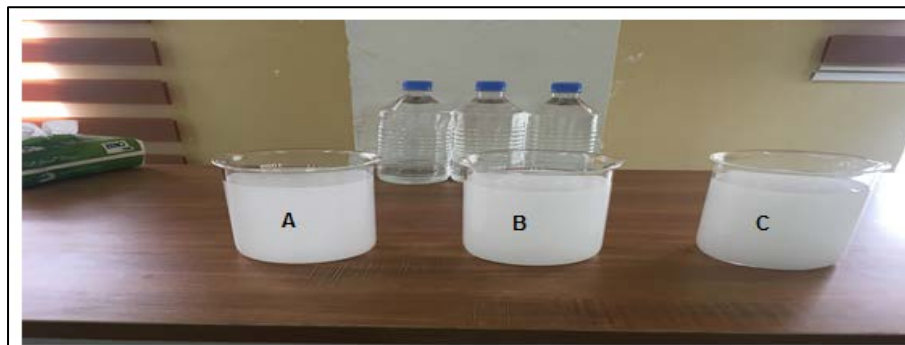


Figure 4: NanofluidSiO₂-H₂O: Vol.conc. A-0.05%, B - 0.075%, C- 0.1%

b. Thermophysical Properties of the Nanofluid SiO₂-H₂O

The physical properties of nanofluid, density ρ_{nf} , specific heat C_{pnf} , Thermal conductivity k_{nf} , and dynamic viscosity μ_{nf} [29,30]. Specifications of thermophysical properties of the nanofluid show in Table 2. According to the below equations:

$$\rho_{nf} = (1 - \varphi)\rho_{bf} + \varphi \rho_{np} \tag{2}$$

$$C_{p,nf} = \frac{(1-\varphi)\rho_{bf} c_{bf} + \varphi \rho_{np} c_{np}}{\rho_{nf}} \tag{3}$$

$$K_{nf} = K_{bf} \left[\frac{K_{np} + 2 K_{bf} + 2 \varphi (K_{np} - K_{bf})}{K_{np} + 2 K_{bf} - \varphi (K_{np} - K_{bf})} \right] \tag{4}$$

$$\mu_{nf} = \frac{\mu_{bf}}{(1-\varphi)^{2.5}} \tag{5}$$

Where:

C_{bf} -specific heat of bas fluid (J/kg.K) , C_{np} -specific heat of nanoparticlas (J/kg.K)

K_{bf} -thermal conductivity of base fluid (w/m.K),

K_{np} -thermal coducivity of nanoparticles (w/m.K),

μ_{bf} - viscosity of base fluid (m²/s)

Table 2: Thermophysical properties of water, nanopartical and nanofluid

Thermophysical properties	H ₂ O	SiO ₂	SiO ₂ +H ₂ O Nanofluid (0.05%)	(SiO ₂ +H ₂ O) Nanofluid (0.075%)	(SiO ₂ +H ₂ O) Nanofluid (0.10%)
Density (Kg/m ³)	1000	2220	1061	1091	1122
Specific heat (J/Kg.k)	4187	745	3827	3663	3433
Thermal conductivity (w/m.k)	0.667	1.4	0.694	0.708	0.722
Viscosity (m ² /s)	0.415e-6	-	0.471e-6	0.504e-6	0.540e-6

3. Thermal Performance

ASHRAE Standard 93-86 [32] suggested implementing the experimental test at different inlet temperatures, after measuring the fluid temperature in the inlet, outlet, water mass flow rate, and specific heat capacity. The useful energy can be determined according to Eq.6. The useful energy could also be indicated in terms of the energy absorbed by absorbent and those lost from the absorber function of removal factor, F_R , solar radiation intensity G_T , cover transmittance factor τ , glass absorbance factor α , and overall heat transfer coefficient U_L . As given by Eq.7. [33]:

$$Q_u = m^* C_p (T_o - T_i) \quad (6)$$

$$Q_u = F_R [G_T (\alpha \tau) A_C - U_L A_C (T_i - T_a)] \quad (7)$$

The thermal efficiency (η) of the FPSC is determined as the energy gained to the energy of fallen solar radiation intensity on the FPSC, The efficiency, combined with Eqs. (8–11) provides the basis for simulation models:

$$F_R = \frac{m^* C_p (T_i - T_a)}{[G_T (\alpha \tau) A_C - U_L A_C (T_i - T_a)]} \quad (8)$$

$$\eta = \frac{Q_u}{A_C G_T} \quad (9)$$

$$\eta = \frac{F_R [G_T (\alpha \tau) A_C - U_L A_C (T_i - T_a)]}{A_C G_T} \quad (10)$$

$$\eta = F_R \left[\alpha \tau - \frac{U_L [T_i - T_a]}{G_T} \right] \quad (11)$$

The collector efficiency, according to Eq. (11), maybe expressed as a straight line [33]. From the average data plotted against $(T_i - T_a)/G_T$, this line intersects the efficiency axis (vertical) at a point of $F_R (\tau \alpha)$. The collector efficiency, at this point, will reach its peak value, and the collector inlet temperature will be equivalent to the ambient temperature. $F_R (\tau \alpha)$ parameter is known as the “absorber energy parameter”. The slope of the straight line is equal to $F_R U_L$ and expressed how to remove the energy from the FPSC. Also, it is known as the “removed energy parameter”.

4. Experimental Setup and Testing Rig

The experiments were carried out during March-April 2019. The FPSC's performance has

experimented with a volume fraction of (0.05%, 0.075%, and 0.10%) SiO_2 + water nanofluid and varying flow rates 10 L/h, 15 L/h, and 20 L/h, and the tilt angle of the collector was 33° . The storage tank is made up of plastic, having a capability of 10 liters. The experimental test set up includes the solar collector, closed working fluid system, and appropriate measuring devices. The working fluid system includes a tank, pay pass pipes system, and simple manual valves utilized to regulate the flow rate of working fluid. The flow rate may be measured using a flow meter. Glass wool insulation is used on the storage tank to protect it from heat loss. The pump is mounted inside the storage tank in order to circulate the working fluid. Moreover, the pump is also mounted inside the storage tank to avoid settling nanoparticles. A thermometer is mounted at both ends of the absorber tube, the inlet, and outlet, for measuring the inlet and outlet fluids temperatures. A solar power meter was utilized to measure solar radiation intensity. The manual tracking mechanism from (East-West) direction has been used in the experiment to follow the position of the sun during the day.

5. Results and Discussion

The experimental tests were conducted to collect the results. The results include the temperature variation, useful heat, solar collector efficiency, and effect of the various mass flow rate of fluid passing through the FPSC on its performance when employing distilled water or a $\text{SiO}_2 + \text{H}_2\text{O}$ nanofluid. All data had been tested in the quasi-steady-state condition. Collector tests have been taken place from 11 AM to 2 PM. The experimental results are presented in the form of graphs and tables describing the temperature variation, useful heat gain, and efficiency of solar collectors.

I. Variation of temperature rise with inlet temperature

The influence of nanofluid type on the outlet-inlet temperature difference (DT) of the FPSC is demonstrated in Figures (4-6) at the mass flow rate (10, 15 and 20 L/h) for water and nanofluids ($\text{SiO}_2 + \text{H}_2\text{O}$) with volume fraction concentration of (0.05, 0.075 and 0.1%) and distilled water, respectively. The experimental results indicated that increasing the average temperature differences between 15, 21, and 30 % for volume fraction 0.05, 0.075, and 0.1%, respectively, as

compared to distilled water. Enhancing the heat transfer of the nanofluids is attributed to the enhanced thermophysical properties such as thermal conductivity and heat transfer coefficient caused by adding the SiO₂ nanoparticles to water. In addition to the above reason, it was noted that adding nanoparticles to the water has many advantages: (a) The heat capacity of the water is decreased so that less energy is required for the nanofluid in comparison with water; in other words, the temperature difference of the nanofluids is larger than that of water if the same amount of heat is provided. (b) The heat transfer area is increased by mixing a little amount of the nanoparticles with the base fluid (water). (c) The mass migration phenomenon of the nanoparticles

in the nanofluid working media further improves the heat transfer enhancement, (d) Diffusion and relative movement of nanoparticles close to the wall of the tube still cause a quick heat transfer from the wall to the nanofluid [34]. The outlet-inlet temperature difference (DT) with the increase of flow rate are shown in Figure 7. It is shown that increasing the flow rate causes the DT to decrease. It is found, at low flow rates, the behavior of the pure H₂O and SiO₂+H₂O nanofluid were identical; nevertheless, at a higher value of flow rate, the DT line slope of the nanofluid was less than that of the pure water. Consequently, the collector based on the SiO₂+H₂O nanofluid has preferable thermal behavior than with pure water.

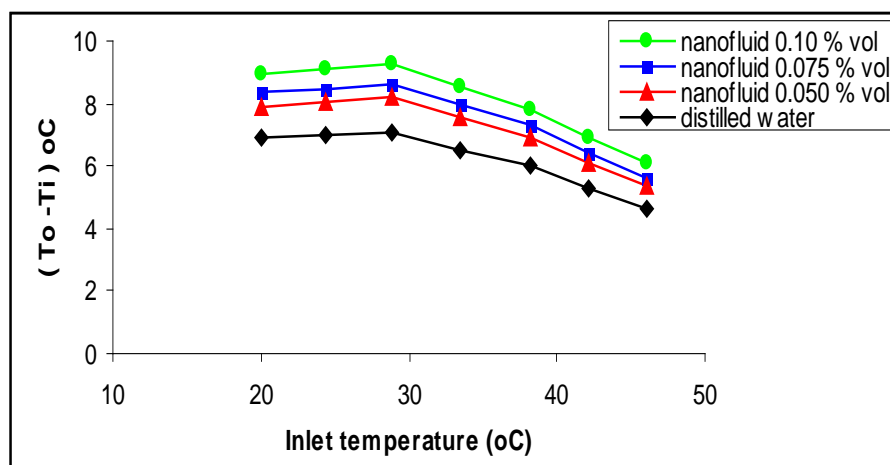


Figure 4: Temperature variation of inlet and outlet solar collector for (SiO₂ + DW) at various values of (φ%) and mass flow rate 10 L/h

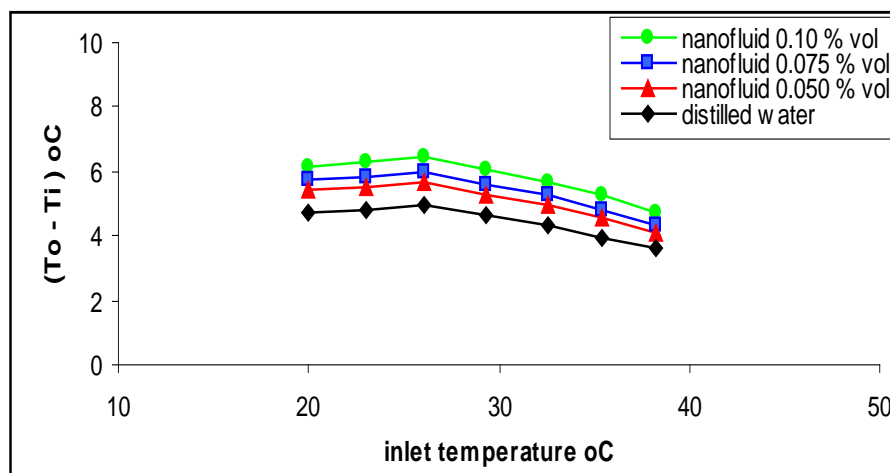


Figure 5: Temperature variation of inlet and outlet solar collector for (SiO₂ + DW) at various values of (φ%) and mass flow rate 15 L/h

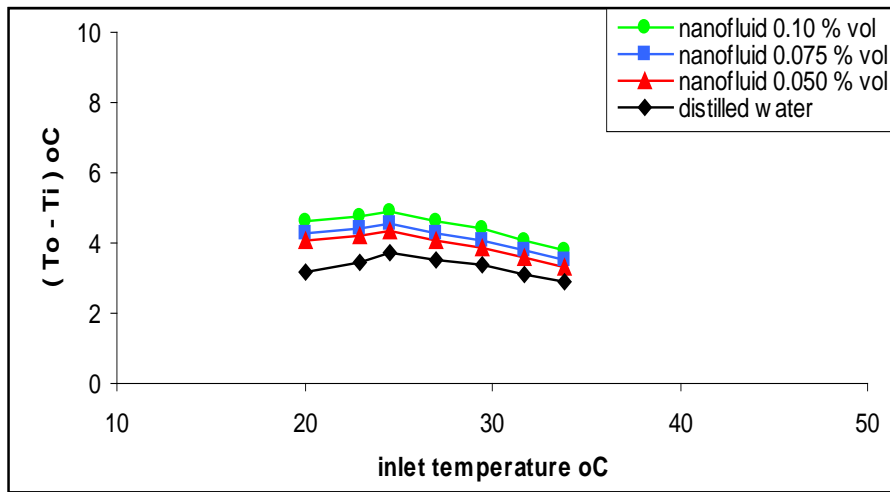


Figure 6: Temperature variation of inlet and outlet solar collector for (SiO₂ + DW) at various values of (ϕ %) and mass flow rate 20 L/h

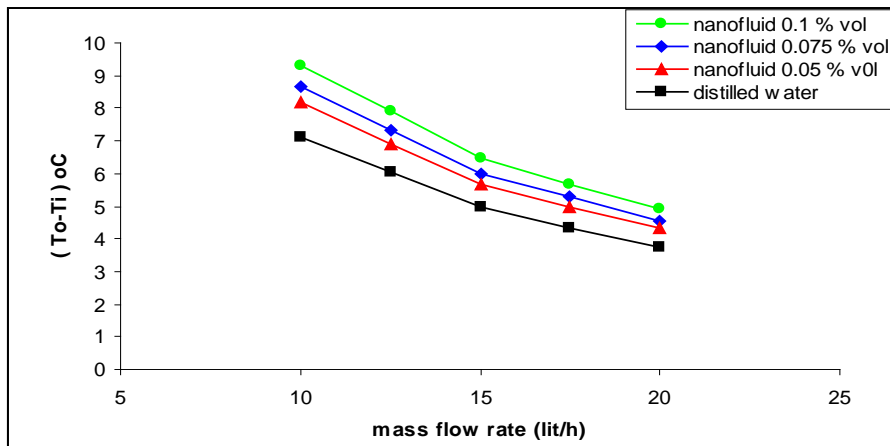


Figure 7: Difference comparison between maximum (inlet & outlet) temperature versus mass flow rate for (SiO₂ + DW) at different (ϕ %)

II. Variation of useful heat gain with inlet temperature

- Figures (8 – 10) are shown that the useful heat gains for FPSC at different inlet temperature,

rates of flow (10, 15 and 20 L/h) and ϕ (0.05, 0.075 and 0.1%vol). The collector based on nanofluids (SiO₂ + DW) at 0.1% vol offered better performance when compared with distilled water.

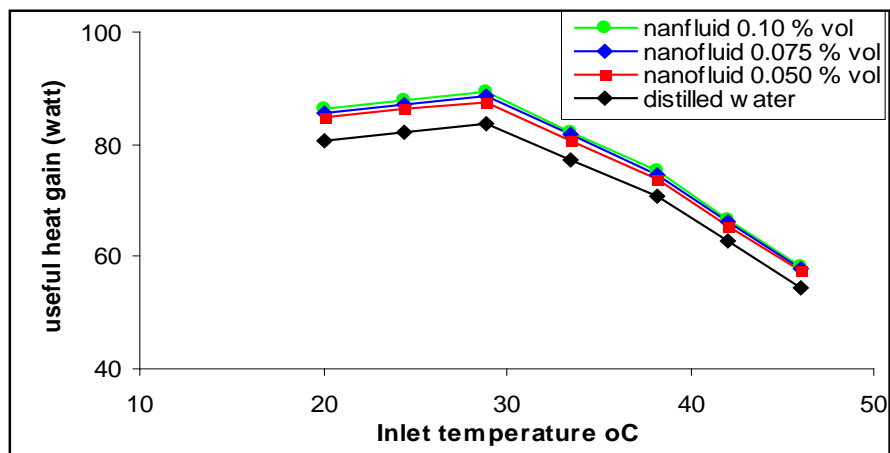


Figure 8: Useful heat gain variation of solar collector for (SiO₂ + DW) at different (ϕ %) and mass flow rate 10 L/h

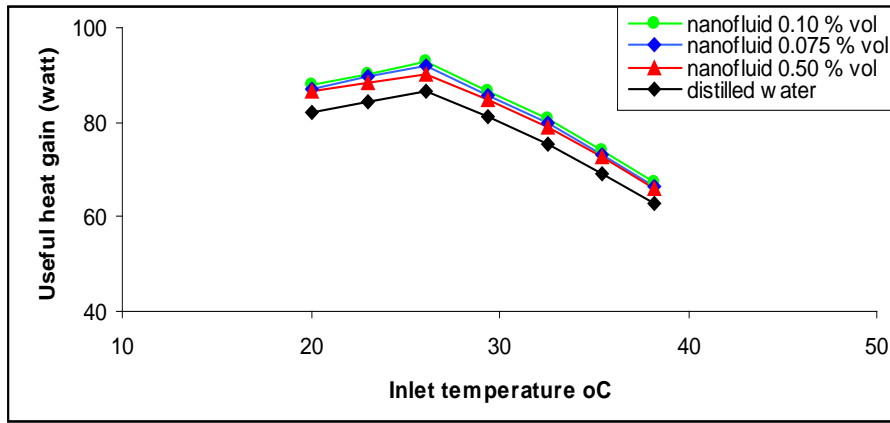


Figure 9: Useful heat gain variation of solar collector for (SiO₂ + DW) at different (φ %) and mass flow rate 15 L/h

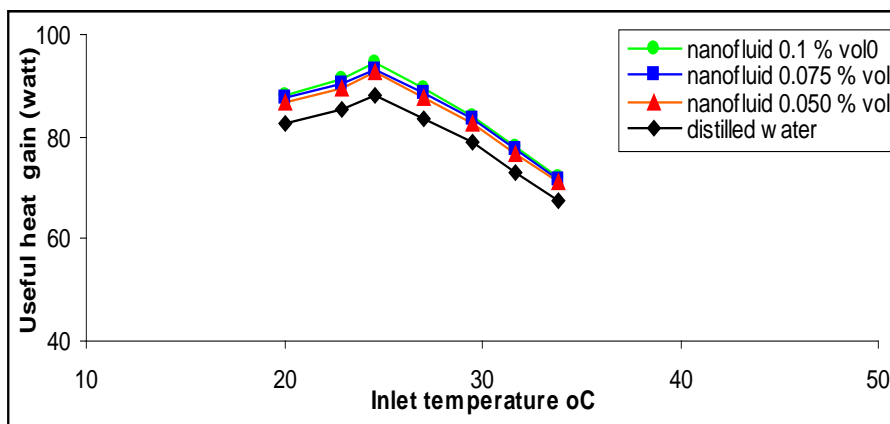


Figure 10: Useful heat gain variation of solar collector for (SiO₂ + DW) at different (φ %) and mass flow rate 20 L/h

III. Efficiency variation with $(T_i - T_a)/G_T$

Figures (11-13) demonstrate the influence of nanofluid volume fraction on the FPSC for different values of volume fraction (φ %) of 0.05, 0.075, and 0.1% at several values mass flow rate of 10 L/h, 15 L/h, and 20 L/h, respectively. The solar collector efficiency with nanofluid is displayed versus the temperature parameters, $[(T_i - T_a)/G_T]$. As demonstrated in Figures (11-13), the efficiency of the FPSC, SiO₂ nanofluid has a large value depends on volume fraction. This conclusion can detect by finding the value of the absorbed energy parameter $F_R(\tau\alpha)$ and removed energy parameter, $F_R U_L$ for SiO₂ nanofluid in Table 3. As demonstrated in Figure 11 for the flow rate of 10 L/h. The absorbed energy parameter, $F_R(\tau\alpha)$ values for SiO₂+H₂O nanofluid, is more than water by 3.6%, 4.4%, and 5.6% for φ %(0.05, 0.075, and 0.1%), respectively. However, removing energy parameter, $F_R U_L$ values for SiO₂+H₂O nanofluid rise by 2.5%, 2.6% and 3.6% for φ % (0.05, 0.075, and 0.1%) with respect to water. Based on Figure 12 going up in the $F_R(\tau\alpha)$ values for the

mass flow rate of 15 L/h is 4.3%, 5.3% and 6.7% for φ % (0.05, 0.075 and 0.1%), respectively, and increasing in values of $F_R U_L$ is 2.3%, 3.7% and 4.1% for (φ %) (0.05 ,0.075 and 0.1%) respectively, comparing to water. Figure 13 showed the values of $F_R(\tau\alpha)$ and $F_R U_L$ for the flow rate of 20 L/h. Values of $F_R(\tau\alpha)$ is raised by 4.4% , 5.6% and 7.3% for φ % (0.05 ,0.075 and 0.1) , respectively. It is observed that the gain in values of $F_R U_L$ for SiO₂nanofluid increased by 1.3%, 3.9%, and 11.9% for φ % (0.05, 0.075, and 0.1%) respect to water. The study of φ % of nanofluid on the FPSC efficiency is complex. It has been noted that higher φ % at 0.1% is absorbed and more energy removed than other φ % of 0.05, 0.075%, and pure water as it has the peak values of $F_R(\tau\alpha)$ and $F_R U_L$ for all mass flow rate of nanofluids. The explanation of that is as the volume fraction increased, the thermal conductivity of fluid rose because more particles were added. However, the collector efficiency does not depend only solely on the values of $F_R(\tau\alpha)$ and $F_R U_L$ but also on the dropped temperature coefficient $[(T_i - T_a)/G_T]$. The

collector efficiency at a volume fraction of nanoparticles ϕ % of 0.075, and 0.05% got higher as the value of $[(Ti-Ta)/GT]$ rises. The collector efficiency in the case of water at the highest values of $[(Ti-Ta)/GT]$ becomes the maximum. The sequence was the same whatever the mass flow as, shown in Figures (11-13).

The lower $[(Ti-Ta)/GT]$ values could be due to the increase in solar radiation or by reducing the temperature difference. Hence, the higher ϕ % of nanofluid is considered useful because it absorbed more heat than others. Also, fewer particles tend to agglomerate comparing to the lower volume ϕ % nanofluid. The microwatts of heat transfer increased as the collision of particles raised. Based on these reasons, the efficiency of the solar collector increased with the rising of the volume fraction. On the other hand side, higher viscosity of nanofluids and full thickness of the boundary

the layer was found when the $[(Ti-Ta)/GT]$ values increased because of the rise in the average fluid temperature. At the same time, solar radiation will decrease, because causing a decrease in absorbent energy and increasing heat loss. Hence, less performance and lower

efficiency were detected as the heat transfer rate reduced [35]. All of the above explanation clarifies the fact that solar collector efficiency has a noticeable depend on the value of $[(Ti-Ta)/GT]$. Since the slopes of the models are negative, it can notice that the increasing $(Ti-Ta)$ makes the efficiency equal to zero.

Diffusion and relative movement of nanoparticles near the tube wall causes fast heat transfer from the wall to nanofluid [34]. The slopes for the nanofluids became steeper as s compared with the water, which demonstrates the influence of utilizing the nanofluids in enhancing the heat removal factor (F_R) of the solar collector. Raising the mass flow rate values or employing nanofluids instead of basic fluid are the methods used to increase the efficiency factor of the collector via increasing the heat transfer coefficient inside the tube [33]. The collector efficiency is in the near range in both coolants. The SiO_2+H_2O nanofluid is more efficient than pure water, with a small variation, mainly since that the thermal conductivity of the SiO_2 is not so bigger than water [19,34,35]. The values of $F_R U_L$ and $F_R (\tau\alpha)$ of the FPSC for water and nanofluid are listed in Table 3

Table 3: $F_R U_L$ and $F_R (\tau\alpha)$ of the FPSC for distilled water and nanofluids

Coolant	(ϕ %) vol	m^*L/h	$F_R (\tau\alpha)$	$- F_R U_L$
Water	-	10	0.6481	4.5275
	-	15	0.6497	4.5476
	-	20	0.6522	4.6266
Nanofluid (SiO_2+DW)	0.05	10	0.6717	4.6424
	0.05	15	0.6782	4.6562
	0.05	20	0.6808	4.6895
Nanofluid (SiO_2+DW)	0.075	10	0.6769	4.6480
	0.075	15	0.6845	4.7176
	0.075	20	0.6890	4.8087
Nanofluid (SiO_2+DW)	0.1	10	0.6864	4.6926
	0.1	15	0.6938	4.7361
	0.1	20	0.7001	5.1817

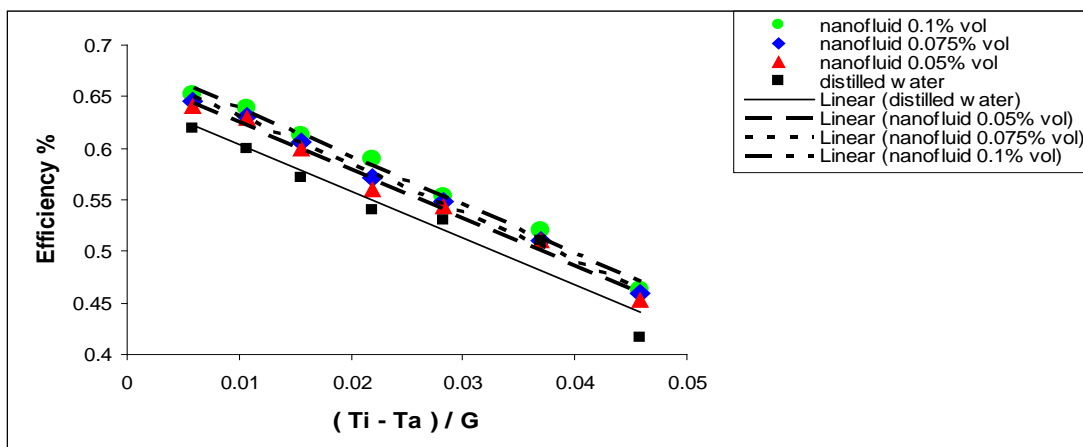


Figure 11: Collector efficiency at different (φ %) and flow rate 10 L/h for nanofluid (SiO₂ +DW)

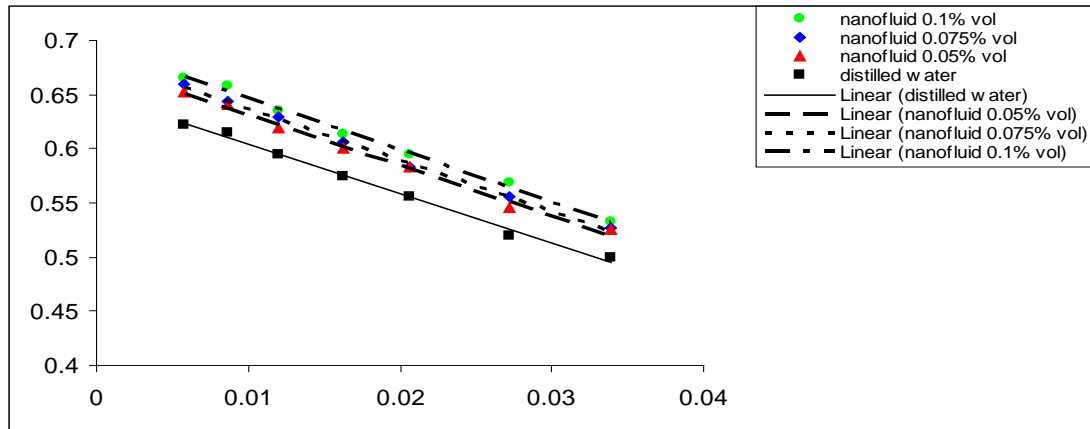


Figure 12: Collector efficiency at different (φ %) and mass flow rate 15 L/h for nanofluid (SiO₂ +DW)

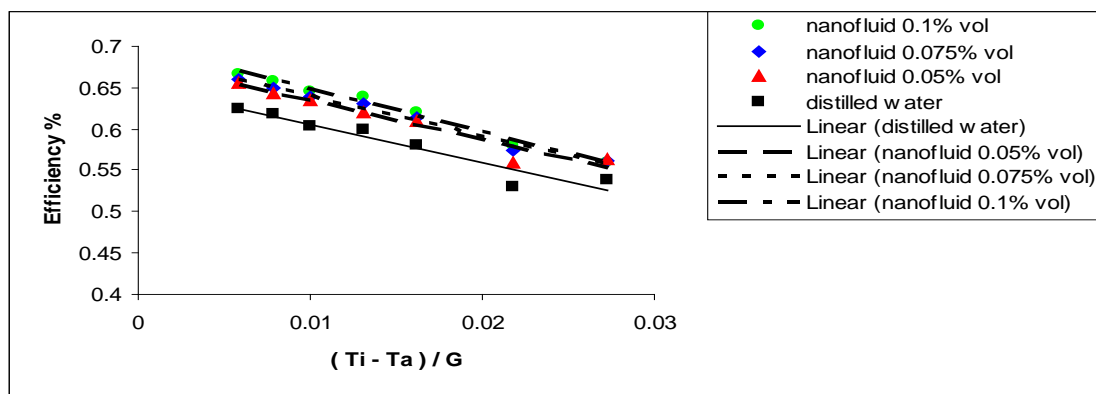


Figure 13: Collector efficiency at different (φ %) and mass flow rate 20 L/h for nanofluid (SiO₂ +DW)

IV. Flow rate effect on the efficiency

The effect of the working fluid flow rate on the FPSC efficiency had been tested. Both water and nanofluid had been tested at various flow rates for evaluating their impact on collector performance. The variation of the FPSC efficiency versus the mass flow rates of (10, 15, and 20 L/h) for water and nanofluid, with a mass fraction of 0.05, 0.075, and 0.10 % are shown in Figure 14. It is seen that the collector efficiency increases in the flow rate for coolants. The researchers C. Cristofari et al. [36] and A. Minsta et al. [37] studies the impact factor of the value of flow rate, the number of Reynolds, and heat transfer rate on the FPSC

performance. Figure 14 clarifies that the efficiency of the solar collector was greatly elevated by using the nanofluid more than distilled water. The interpretation of this trend goes back to that average velocity and number of Reynolds of coolant had been increased with the increase of rate of the flow. Therefore, the motion rate, especially the Brownian motion and motion of the particles in SiO₂+H₂O coolant nanofluid, are increasing according to the flow rate and the velocity of nanofluid. The movement of nanoparticles in the SiO₂+H₂O nanofluid leads to more heat transfer and the later dramatic rise the solar collector efficiency compared to water use [38,39].

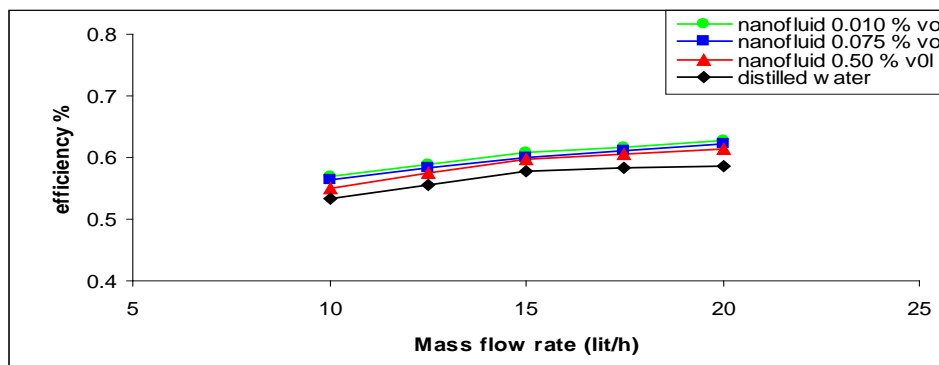


Figure 14: Variation of mass flow rate with efficiency at different (ϕ) of nanofluid (SiO₂ +DW)**V. Comparison with previous studies**

Many researchers studied the performance of the FPSC using SiO₂+water. Table 4 demonstrates the summary of the experimental studies and their results. The results obtained from these studies on the effect of SiO₂ almost identical to the results in

the present study. Nevertheless, there is a difference between the SiO₂ results and that in this study. The difference is resulting from utilizing different amounts of SiO₂ and applying the tests at various values of flow rate.

Table 4: A summary of experimental studies on flat-plate solar collectors using (SiO₂ water) Nanofluids

Faizal et al. [19]	SiO ₂ + water	0.2 and 0.4 vol%	15 nm	- Efficiency increases by 23.5 %
Saleh et al. [40]	SiO ₂ / EG + water	0.5,0.75, & 1 vol%	40nm	Efficiency increases with range of (4 – 8) %
Sujit et al. [18]	Al ₂ O ₃ , CuO, SiO ₂ , TiO ₂ , Graphene, MWCNTs; (water as a base fluid)	0.25-2 vol%	(7 - 45) nm	Maximum efficiency enhanced by 23.47% (compared to water) obtained by MWCNTs/water, and the minimum value by 5.74% for SiO ₂
Aminreza et al. [41]	SiO ₂ /water	1wt %	12nm	- Thermal efficiency enhanced by using nanofluid

6. Conclusions

The highlights of the study may be summarized as follows:

- The maximum thermal efficiency was about 70 % as decreased temperature parameter, [(Ti-Ta)/GT] is equal to zero at volume fraction 0.10 % and flow rate of 20 L/h. The highest rise in the absorbed energy parameter $F_R(\tau\alpha)$ was 7.3%, as compared with pure water. Note that the difference is not that big. This produces mainly due because of the fact that the thermal conductivity of SiO₂ and SiO₂+H₂O is not much bigger than in water.

- The maximum increase in $F_R U_L$ is 11.9 at a volume fraction 0.10% and a flow rate of 20 L/h. The variation in the absorbed energy parameter $F_R(\tau\alpha)$ varies from 4.4% to 7.3%, while in removed energy parameter $FRUL$, they vary from 1.3% to 11.9% as compared with the water case. The collector efficiency is directly proportional to both flow rate and volume fraction of nanoparticles.

- For broad operating conditions, the performance of FPSC is raised using the SiO₂+H₂O nanofluid compared to that using water. One is the highest temperature related to using the nanofluid in the collector can be influenced by the specific heat of the working fluid. Nanoparticles and nanofluids have lower specific heat than water. Therefore, less heat required raising the temperature of nanofluids, which makes the resulting output

temperature, and thus, thermal efficiency becomes the higher.

Acknowledgements

To our knowledge, this is the first study, which is searching for the thermal analysis of FPSC using SiO₂-H₂O nanofluid based small aperture area of FPSC of 0.192 m², small values of volume fraction 0.05, 0.075 and 0.1 % and low several mass flow rates 10, 15 and 20 L/h .In order to determine the impact of these parameters on the thermal performance of FPSC.

References

- [1] S. Kalogirou, "Solar thermal collectors and applications," Prog. Energy Combust. Sci., 30, 231–295, 2004.
- [2] S. Riffat, X. Zhao, P.S. Doherty, "Developing a theoretical model to investigate thermal performance of a thin membrane heat-pipe solar collector," Appl. Therm. Eng., 25, 899–915, 2005.
- [3] S. Kalogirou, "Prediction of flat plate collector performance parameters using artificial neural networks," Sol. Energy, 80, 248–259, 2006.
- [4] N. Kumar, T. Chavda, H.N. Mistry, "A truncated pyramid non tracking type multipurpose solar cooker/hot water system," Appl. Energy, 87, 471–477, 2010.

- [5] Z. Chen, S. Furbo, B. Perers, J. Fan, A. Andersen, "Efficiencies of flat plate solar collectors at different flow rates," *Energy Procedia*, 30, 65–72, 2012.
- [6] M. Abdolzadeh, M.A. Mehrabian, "The optimal slope angle for solar collectors in hot and dry parts of Iran," *Energy Sources Part, A* 34, 519–530, 2012.
- [7] J. Duffie, W.A. Beckman, "Solar Engineering of Thermal Processes," 4th ed. Wiley, New York, 2013.
- [8] L.M. Ayompe, A. Duffy, "Analysis of the thermal performance of a solar water heating system with flat plate collectors in a temperate climate," *Appl. Therm. Eng.*, 58, 447–454, 2013.
- [9] S. Choi, Z.G. Zhang, "Anomalous thermal conductivity enhancement in nanotube suspensions," *Appl. Phys. Lett.*, 79, 2252–2254, 2001.
- [10] H. Tyagi, P. Phelan, R. Prasher, "Predicted efficiency of a low-temperature nanofluid-based direct absorption solar collector," *J. Sol. Energy Eng.*, 131, 1–7, 2009.
- [11] R. Taylor, T.P. Phelan, C.A. Otanicar, M. Walker, S. Nguyen, Trimble, R.S. Parsher, "Applicability of nanofluids in high flux solar collectors," *J. Renew. Sustain. Energy*, 3, 023104, 2011.
- [12] D. Han, Z. Meng, D. Wu, C. Zhang, H. Zhu, "Thermal properties of carbon black aqueous nanofluids for solar absorption," *Nanoscale Res. Lett.*, 6, 1–7, 2001.
- [13] T. Yousefi, E. Shojaeizadeh, F. Veysi, S. Zinadini, "An experimental investigation on the effect of MWCNT-H₂O nanofluid on the efficiency of flat-plate solar collectors," *Exp. Therm. Fluid Sci.*, 39, 207–212, 2012.
- [14] T. Otanicar, J. Golden, "Comparative environmental and economic analysis of conventional and nanofluid solar hot water technologies," *Environ. Sci. Technol.*, 43, 6082–6087, 2009.
- [15] P. Phelan, T. Otanicar, R. Parsher, G. Rosengarten, R. Taylor, "Nanofluid-based direct absorption solar collector," *J. Renew. Sustain. Energy*, 2, 033102, 2010.
- [16] T. Yousefi, E. Shojaeizadeh, F. Veysi, S. Zinadini, "An experimental investigation on the effect of Al₂O₃-H₂O nanofluid on the efficiency of flat plate solar collector," *Renew. Energy*, 39, 293–298, 2012.
- [17] O. Mahian, A. Kianifar, A.Z. Sahin, S. Wongwises, "Performance analysis of a minichannel-based solar collector using different nanofluids," *Energy Convers. Manag.*, 88, 129–138, 2014.
- [18] S. Kumar Verma, Arun Kumar Tiwari, Durg Singh Chauhan, "Experimental evaluation of flat plate solar collector using nanofluids," *Energy Conversion and Management*, 134, 103–115, 2017
- [19] M. Faizal, R. Saidur, S. Mekhilef, M.A. Alim, "Energy, economic and environmental analysis of metal oxides nano fluid for flat-plate solar collector," *Energy Conversion and Management*, 76, 162–168, 2013.
- [20] M. Alim, Z. Abidin, R. Saidur, A. Hepbasli, M.A. Khairul, N.A. Rahim, "Analyses of entropy generation and pressure drop for a conventional flat plate solar collector using different types of metal oxide nanofluids," *Energy and Buildings*, 66, 289–296, 2013
- [21] E. Arıkan, Serkan Abbasoglu and Mustafa Gazi, "Experimental Performance Analysis of Flat Plate Solar Collectors Using Different Nanofluids," *sustainability*, 2-11, 2018.
- [22] A. Tiwari, K. Pradyumna Ghosh, P., Sarkar, J., "Solar Water Heating Using Nanofluids—A Comprehensive Overview And Environmental Impact Analysis," *International Journal of Emerging Technology and Advanced Engineering*, 3(Special Issue 3), 221 – 224, 2013.
- [23] J. Golden, O.T., "Comparative environmental and economic analysis of conventional and nanofluid solar hot water technologies," *Environ. Sci. Technol.*, 43, 2015.
- [24] P. Rhushi Prasad, H.V. Byregowda, P.B. Gangavati, "Experiment Analysis of Flat Plate Collector and Comparison of Performance with Tracking Collector," *European Journal of Scientific Research*, Vol.40, No.1, 144 -155, 2010.
- [25] P. Drago, "A simulated comparison of the useful energy gain in a fixed and a fully tracking flat plate collector," *Solar Energy*, 1978.
- [26] Y. Pavel, Gonzalez HJ, Vorobiev YV., "Optimization of the solar energy collection in tracking and non-tracking PV solar system," *Proceedings of the 1st international conference on electrical and electronics engineering, ICEEE*, 2004.
- [27] S. Noor, "Evaluation of experimental performance of flat plate solar collector using different bonding tubes at the absorber plate with tracking system," *MSc. Thesis, Technology University, Baghdad*, 2016.
- [28] P. John and P.D. Shima, "Thermal properties of nanofluids," *Advances in Colloidal and Interface Surface*, vol. 10, no. 4, 30–45, 2012.
- [29] M. Chang, H. Liu, H.S. Tai, "Preparation of copper oxide nanoparticles and its application in nanofluid," *Powder Technology*, Vol. 207, 378–386, 2011.
- [30] T. yousefi, veysi F., Shajaeizadeh E., Zinadini S., "An experimental investigation on effect of Al₂O₃-H₂O nanofluid on the efficiency of flat-plate solar collector," *Renewable energy*, Vol.39, 293–298, 2012.
- [31] F. Javadi S., Sadeghipour S., Saidur R., Boroumandjazi G., R13 ahmati B., Eilas M. M., Sohel M.R., "The effects of nanofluid on thermophysical properties and heat transfer characteristics of a plate heat exchanger," *international communications in heat and mass transfer*, Vol.44, 58–63, 2013.
- [32] ASHRAE Standard 93-86, "Methods of Testing and Determine the Thermal Performance of Solar Collectors," *ASHRAE*, Atlanta, 2003.

- [33] J. Duffie A., & Beckman, W. A., "Solar engineering of thermal processes," Wiley publication, 1991.
- [34] C. Chon and Kihm KD., "Thermal conductivity enhancement of nanofluids by Brownian motion," *Journal of Heat Transfer*, 127, 8, 810, 2005.
- [35] H. Qinbo, Shequan Zeng and Shuangfeng Wang, "Experimental investigation on the efficiency of flat-plate solar collectors with nanofluids," *Applied Thermal Engineering*, 88, 165-171, 2015.
- [36] C. Cristofari, G. Notton, P. Poggi, A. Louche, "Modeling and performance of a copolymer solar water heating collector," *Solar Energy*, 72, 99-112, 2002.
- [37] A. Mintsu, M. Medale, C. Abid, "Optimization of the design of a polymer flat plate solar collector," *Solar Energy*, 87, 64-75, 2013.
- [38] J. Koo, C. Kleinstreuer, "A new thermal conductivity model for nanofluids," *Journal of Nanoparticle Research*, 6, 577-588, 2004.
- [39] Y. Xuan, Q. Li, W. Hu, "Aggregation structure and thermal conductivity of nanofluids," *AIChE Journal*, vol. 49, 1038-1043, 2003.
- [40] S. SalavatiMeibodi, Ali Kianifar, Hamid Niazmand, OmidMahian, and Somchai Wongwises, "Experimental investigation on the thermal efficiency and performance characteristics of a flat plate solar collector using SiO₂/EG-water nanofluids," *Int. Communications in Heat and Mass Transfer*, 65, 71-75, 2015.
- [41] A. Noghrehabadi, Ebrahim Hajidavaloo and Mojtaba Moravej, "Experimental investigation of efficiency of square flat-plate solar collector using SiO₂/water nanofluid," *Case Studies in Thermal Engineering*, 8, 378-386, 2016.